PARAMETER IDENTIFICATION OF THE INTERACTION BODY MODEL USING AVAILABLE MEASUREMENTS

Qingwen Zhang[1,2] – Zheng Li[1,2] – Yu Zhang[1,2*] – Tianjian Ji[3]

[1]Key Lab of Structures Dynamic Behavior and Control of the Ministry of Education, Harbin Institute of Technology, Harbin, 150090, China
[2]Key Lab of Smart Prevention and Mitigation of Civil Engineering Disasters of the Ministry of Industry and Information Technology, Harbin Institute of Technology, Harbin, 150090, China
[3]School of Mechanical, Aerospace and Civil Engineering, The University of Manchester, UK

ARTICLE INFO

Article history
Received: 14.1.2017.
Received in revised form: 9.8.2017.
Accepted: 28.8.2017.

Keywords:
Parameter Identification
The interaction model

DOI: http://doi.org/10.30765/er.40.3.01

Abstract:

This paper determines the parameters of the interaction models based on available published experimental measurements. The masses, damping ratios and stiffnesses of body models are identified by the curve fitting of the measured apparent mass curves from shaking table tests in published biomechanics studies. Then the extracted data are used to identify the parameters of the interaction models. Finally, the eigenvalue analyses of the human-structure models are calculated for comparison. In this identification process, it was identified that the quality of the curve fitting for the interaction model is as good as and even slightly better than the published results. One or two additional conditions for the interaction models would lead to several sets of parameters, but with the result of the continuous model, reasonable parameters have to be applied which can be identified and these parameters could be used in further calculations.

1 Introduction

In recent years, the span lengths of new constructions have been gradually increasing. Also, higher-strength and lighter-weight construction materials have been used in many new structures. As a result, the natural frequencies of the structures reduce to the point where the resonant or near-resonant vibration may be induced by human actions and this, in turn, can lead to unacceptable levels of vibration. Consequently, human-structure interaction needs to be considered when designing new structures excited and/or occupied by people. To research this project, it is important to use an appropriate model of the human body in the study.

The human body can be modelled in various ways with five representations being considered here:
1. Biomechanics models that were developed based on the results of shaking table tests;
2. Conventional models that were developed based on a fixed base and often used in structural vibration;
3. Interaction models that were developed based on a vibrating structure;
4. Continuous models that describe a standing person using continuous stiffness and mass functions;
5. Higher degree of freedom models that require a finite element solution.

This paper uses four biomechanics models (Model 1a, Model 1b, Model 2c and Model 2d) that were developed by Matsumoto and Griffin [1]. The

* Corresponding author, Tel.: +8645186283199; fax: +8645186283097
E-mail address: zhangyuhit@hit.edu.cn

difference between the two models is that Model 1a had a massless support at its base, whereas the bottom structure in Model 1b had a mass M_0.

Another two models have been developed from the SDOF model. The kind of connection between these 2DOF models is that the second DOF is completely independent of the first DOF. The support structure in Model 2c had no mass, whereas the support structure in Model 2d had a mass M_0.

Biomechanics researchers have usually obtained dynamic characteristics of the human body experimentally by placing a person on a shaking table in laboratory conditions. The experimental data were then used to calculate apparent mass $M(f)$ [2]. By curve-fitting to the apparent mass, the dynamic properties of the biodynamic human models were identified [3].

Matsumoto and Griffin studied the apparent mass of standing human bodies on a shaking table that was subjected to vertical vibration from a 1-m stroke electro-hydraulic vibrator [3]. 12 male subjects were subjected to random vertical vibration in the frequency range between 0.5 and 30 Hz at vibration magnitudes between 0.125 and 2.0 ms^{-2} r.m.s. It was found that the resonance frequency of the apparent mass in a normal posture decreased from 6.75 Hz to 5.25 Hz when the vibration magnitude increased from 0.125 to 2.0 ms^{-2} r.m.s. Their further work provided discrete models to represent a standing person, including two SDOF models, two 2DOF models, and two other models, each consisting of two SDOF systems [1]. The parameters for the models were determined by comparing the measured and calculated apparent masses.

Two interaction models are used in the following sections. The derivation of these models is represented in detail in section 3 [4, 5].

Based on an anthropomorphic model, a continuous human body model including seven segments of a standing human body is developed [6]. The two stiffnesses of the upper and lower body are identified using two available measured natural frequencies of a standing body. The modal properties of the standing body are also determined and linked to those of discrete body models [6-9]. To help understand the model of a standing human body in vertical vibration, parameters of the continuous model need to be determined correctly. In this paper, the parameters of the body model are determined using available published experimental measurements. Section 2 provides the method and criteria for the parameter identification. Section 3 identifies the parameters of the interaction model. A comparison of human-structure models is given in Section 4. Section 5 gives the concluding remarks and summarizes the findings from this study.

2 Verification of the method

The parametric identification method proposed by Matsumoto and Griffin is tested here to determine the basic parameters of Model 1a, 1b, 2c, 2d [1]. Optimised parameters are obtained by a non-linear parameter search method, based on the Nelder–Mead simplex method, which is provided within MATLAB (MathWorks Inc.). The Nelder–Mead method is a commonly used nonlinear optimization technique, which is a well-defined numerical method for twice differentiable problems. The initial values of the natural frequencies were selected as 3, 4, or 5 Hz for one of the mass-spring systems, and 10 or 15 Hz for the second mass-spring system. The selection of different initial parameters in the parameter research results in the same sets of optimum parameters for all the models.

The apparent mass for the four models is:

Model 1a:

$$M_{1a}(i\omega) = \frac{M_1(iC_1\omega + K_1)}{(-M_1\omega^2 + iC_1\omega + K_1)} \tag{1}$$

Model 1b:

$$M_{1b}(i\omega) = \frac{M_1(iC_1\omega + K_1)}{(-M_1\omega^2 + iC_1\omega + K_1)} + M_0 \tag{2}$$

Model 2c:

$$M_{2c}(i\omega) = \frac{M_1(iC_1\omega + K_1)}{(-M_1\omega^2 + iC_1\omega + K_1)} + \frac{M_2(iC_2\omega + K_2)}{(-M_2\omega^2 + iC_2\omega + K_2)} \tag{3}$$

Model 2d:

$$M_{2d}(i\omega) = M_{2c} + M_0 \tag{4}$$

The apparent masses are calculated using Eq. 1~4 for each of the four models were compared with the measured apparent mass curve of standing subjects. The results demonstrate that the method presented is

valid which will be used for identifying the parameters of the interaction models [1].

3 Parameter identification for the interaction models

3.1 Model 1c

The parameters of the interaction model are identified in this section.

The differences between Model 1b (Fig. 1(b)) and Model 1c (Fig. 2(a)) are:

- A mass device is present in Model 1c with a value of $M_{H1}-M_{H11}$, which is defined in Section 2.2.
- The sum of the top and bottom masses equals the total body mass in Model 1c, while the total mass in Model 1b is 0.0955+0.955=1.05 times the body mass.

The apparent mass of Model 1c, the interaction model, can be given theoretically using complex functions in a similar form to those for Model 1a, 1b, 2c and 2d.

The basic equation of motion of Model 1c:

$$\begin{bmatrix} M_{H0}+M_{H11}-2M_1 & M_{H1}-M_{H_{11}} \\ M_{H1}-M_{H11} & M_{H11} \end{bmatrix} \begin{Bmatrix} \ddot{x}_s \\ \ddot{x}_1 \end{Bmatrix} + \begin{bmatrix} C_H & -C_H \\ -C_H & C_{H1} \end{bmatrix} \begin{Bmatrix} \dot{x}_s \\ \dot{x}_1 \end{Bmatrix} + \begin{bmatrix} K_H & -K_H \\ -K_H & K_H \end{bmatrix} \begin{Bmatrix} x_s \\ x_1 \end{Bmatrix} = \begin{Bmatrix} P_s(t) \\ 0 \end{Bmatrix} \tag{5}$$

Equation 5 can be written as:

$$\begin{aligned} &\left(M_{H0}+M_{H11}-2M_{H1}\right)\ddot{x}_s \\ &+\left(M_{H1}-M_{H11}\right)\ddot{x}_1 - C_H\left(\dot{x}_1-\dot{x}_s\right) \\ &-K_H\left(x_1-x_s\right)=P_s(t) \end{aligned} \tag{6}$$

$$\begin{aligned} &\left(M_{H1}-M_{H11}\right)\ddot{x}_s + K_H\left(x_1-x_s\right) \\ &+C_H(\dot{x}_1-\dot{x}_s)+K_H\left(x_1-x_s\right)=0 \end{aligned} \tag{7}$$

Adding Equation 7 to Equation 6, and dividing both sides of the equation by $\ddot{x}_s$, gives:

$$\frac{P_{S(t)}}{\ddot{x}_S}=M_{H1}\frac{\ddot{x}_1}{\ddot{x}_S}+M_{H0}-M_{H1} \tag{8}$$

Equation 7 can be rewritten as follows:

$$\begin{aligned} &-M_{H11}\omega^2 Ae^{i\omega t}+iC_H\omega Ae^{i\omega t} \\ &+K_H Ae^{i\omega t}=(M_{H1}-M_{H11})\omega^2 Be^{i\omega t} \\ &+iC_H Be^{i\omega t}+K_H Be^{i\omega t} \end{aligned} \tag{9}$$

The absolute motion is:

$$x_1=Ae^{i\omega t} \qquad x_S=Be^{i\omega t} \tag{10}$$

Substituting Equation 10 into Equation 9 gives:

$$\begin{aligned} &-M_{H11}\omega^2 Ae^{i\omega t}+iC_H\omega Ae^{i\omega t} \\ &+K_H Ae^{i\omega t}=\left(M_{H1}-M_{H11}\right)\omega^2 Be^{i\omega t} \\ &+iC_H\omega Be^{i\omega t}+K_H Be^{i\omega t} \end{aligned} \tag{11}$$

Equation 11 can be re-arranged as:

$$\begin{aligned} &\frac{\ddot{x}_1}{\ddot{x}_S}=\frac{Ae^{i\omega t}}{Be^{i\omega t}} \\ &=\frac{\left(M_{H1}-M_{H11}\right)\omega^2+iC_H\omega+K_H}{-M_{H11}\omega^2+iC_H\omega+K_H} \end{aligned} \tag{12}$$

$$\begin{aligned} &M_{1C}\left(i\omega\right)= \\ &\frac{M_{H1}\left(\left(M_{H1}-M_{H11}\right)\omega^2+iC_H\omega+K_H\right)}{\left(-M_{H11}\omega^2+iC_H\omega+K_H\right)} \\ &+M_{H0}-M_{H1} \end{aligned} \tag{13}$$

$$K_H=M_{H11}(2\pi f_1)^2 \tag{14}$$

$$C_H=2\xi M_{H11}(2\pi f_1) \tag{15}$$

Substituting Equation 14 and 15 into Equation 13 gives:

$$M_{1C}(i\omega)=\frac{M_{H1}((M_{H1}-M_{H11})(2\pi f)^2}{(-M_{H11}(2\pi f)^2+i2\xi_1 M_{H11}(2\pi f_{H1})(2\pi f)+M_{H11}(2\pi f_{H1})^2)} + \frac{+i2\xi_1 M_{H11}(2\pi f_{H1})(2\pi f)+M_{H11}(2\pi f_{H1})^2)}{(-M_{H11}(2\pi f)^2+i2\xi_1 M_{H11}(2\pi f_{H1})(2\pi f)+M_{H11}(2\pi f_{H1})^2)}+M_{H0}-M_{H1} \quad (16)$$

Wei and Griffin suggest that the reason why the non-vibration mass M_{H0} contributes only mass is that it represents the effect of other models that are above the frequency range of interest [10]. To determine the parameters, M_{H0} must be hypothesized. As $M_{1c}(i\omega)$ is the normalized mass, M_{H0} =1. There are four unknown parameters $M_{H0}, M_{H1}/M_{H11}, \xi_{H1}$ f_{H1} in Equation 16. The Case 1 is considered following the same treatment of Matsumoto and Griffin [1].

Case 1: $M_{H0}-M_{H1}=10\%M_{H1}$

If the bottom mass $M_{H0}-M_{H1}$ is assumed to be 10% of the upper mass M_{H1}, which follows the treatment of Matsumoto and Griffin, the parameters are as shown in Table 1.

Using these parameters, the first diagonal element in the mass matrix in Equation 5 becomes

$M_{H0}+M_{H11}-2M_{H1}$

=1+0.7933-2×0/9090=-0.0247<0.

Physically the diagonal element in the mass matrix should be positive. Hence this is not a valid case.

Due to the invalid results following the treatment of Matsumoto and Griffin, a new treatment is suggested here. Both the numerator and denominator of Equation 16 are divided by M_{H11}, Equation 16 becomes:

$$M_{iC}(i\omega)=\frac{M_{H1}((\frac{M_{H1}}{M_{H11}}-1)(2\pi f)^2+i2\xi_{H1}(2\pi f_{H1})(2\pi f)+(2\pi f_{H1})^2)}{(-(2\pi f)^2+i2\xi_{H1}(2\pi f_{H1})(2\pi f)+(2\pi f_{H1})^2)}+1-M_{H1} \quad (17)$$

There are four unknown parameters M_{H1}/M_{H11}, M_{H1}, ξ_{H1}, f_{H1} in Equation 17.

It is noted in the identification, that the results are dependent on the initial values of M_{H1} and M_{H11}. If ξ_{H1} and f_{H1} are given before the identification, the number of unknown parameters in Equation 17 reduces from four to two, but the identified results are still dependent on the initial values of M_{H11} and M_{H11}. When the ratio M_{H1}/M_{H11} is given, the results become stable and do not change with the initial values M_{H1} and M_{H11}.

Table 1. Identified parameters of Model 1c for case 1

	K_H	C_H	M_{H1}	M_{H11}	f_{H1}	ξ_{H1}
$M_{H0}-M_{H1}$=10%M_{H1}	1052	41.5	0.9090	0.7933	5.80	0.7176

The apparent mass of model 1b can be rewritten as follows:

$$M_{1b}(i\omega)=\frac{M_1\left(i2\xi_{H1}(2\pi f_{H1})(2\pi f)+(2\pi f_{H1})^2\right)}{\left(-(2\pi f)^2+i2\xi_{H1}(2\pi f_{H1})(2\pi f)+(2\pi f_{H1})^2\right)}+M_0 \quad (18)$$

Comparing Equation 17 and 18, it can be noted that an additional item, $(M_{H1}/M_{H11}-1)(2\pi f)^2$, is present in the numerator in Equation 17. When the ratio M_{H1}/M_{H11} is given, the format of the two equations becomes the same. This may explain the reason why the identified results are not stable unless

the ratio M_{H1}/M_{H11} is given.

Case 2: The ratio of M_{H1}/M_{H11} is given in the range of 1.1 and 1.8.

Several trial ratios M_{H1}/M_{H11} between 1.1~1.8 are given for the identification process. The ratio of M_{H1}/M_{H11}=1.36 is also included, which is based on the continuous body model [4]. The identified parameters of the interaction model are provided in Table 2 for the given ratios of M_{H1}/M_{H11}.

Table 2. Identified parameters of Model 1c for Case 2

M_{H1}/M_{H11}	K_H	C_H	M_{H1}	M_{H11}	f_{H1}	ξ_{H1}	M_{H1}^2/M_{H11}
1.8	426	16.8	0.579	0.321	5.80	0.717	1.04
1.7	478	18.8	0.613	0.360	5.80	0.717	1.04
1.6	539	21.3	0.651	0.409	5.80	0.717	1.04
1.5	614	24.2	0.694	0.463	5.80	0.717	1.04
1.4	705	27.8	0.744	0.531	5.80	0.717	1.04
1.36	**747**	**29.4**	**0.766**	**0.563**	**5.80**	0.717	1.04
1.3	817	32.2	0.801	0.616	5.80	0.717	1.04
1.2	959	37.8	0.868	0.723	5.80	0.717	1.04
1.1	1141	45.0	0.947	0.861	5.80	0.717	1.04

Figure 1 compares the measured and identified normalized apparent mass and phase against frequency of Model 1b and 1c, where the solid lines indicate the measurements and the dashed lines indicate the theoretical predictions based on the identified parameters when M_{H1}/M_{H11}=1.36.

The results in Table 2 and Fig. 1 show that:

- The first natural frequency f_{H1} and the damping ratio of ξ_{H1} the interaction model does not change with the ratio M_{H1}/M_{H11}.
- The parameter $M_{H1}{}^2/M_{H11}$ is a constant (1.04), when M_{H1}/M_{H11} is changed during the identification.

The model parameters, natural frequencies and damping ratios, were optimized through minimizing the following error function:

$$err = \sqrt{\frac{1}{n}\sum_{i=1}^{n}\left|M_m(i\Delta f) - M_c(i\Delta f)\right|^2} \qquad (19)$$

where M_m is the measured apparent mass and M_c is the calculated apparent mass, Δf is the frequency increment and 0.1 Hz is taken in the curve fitting process.

Table 3 summaries the identified results of Model 1b and Model 1c separately.

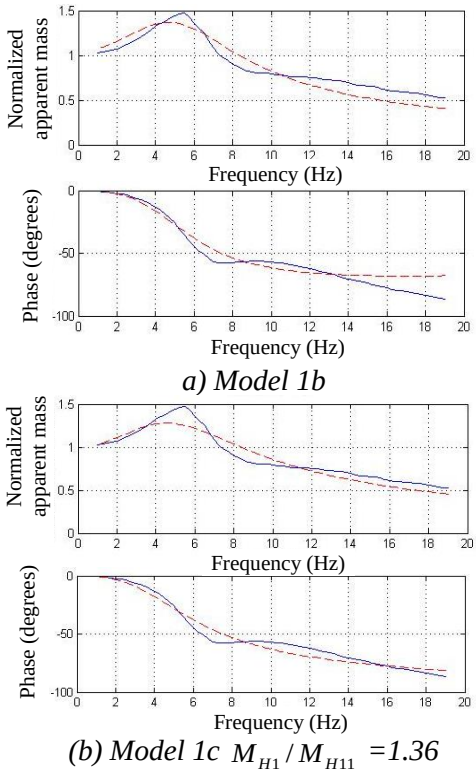

a) Model 1b

(b) Model 1c M_{H1}/M_{H11} *=1.36*

Figure 1. Comparison of the normalized apparent masses and phase between Models 1b and 1c

The results in Table 3 show that:

- The frequency ratio for the continuous body model is the smallest among the four models and is closest to the ratio of the measured natural frequencies [4].

The continuous body model has the same fundamental natural frequency as the measured one while its second natural frequency is 10% larger than the measurement. f_{H1} of Model 1c is smaller than f_{H1} of Model 1b while ξ_{H1} of Model 1c is greater than ξ_{H1} of Model 1b.

- The interaction model (Models 1c) provides smaller fitting errors than Models 1b, which may indicate that the interaction model is a more appropriate representation of a standing human body than Model 1b.
- As Model 1b and 1c are physically different, it is expected that the basic parameters of the two models would have some differences although they are determined from the same sets of measurements.
- The mass device in Model 1c decreases the natural frequency, and increases the damping ratio of the human body model, because this is the only difference between Model 1b and 1c.

Table 3. Identified parameters of Model 1b and 1c

	f_{H1} (Hz)	ξ_{H1}	error
Model 1b	5.87	0.612	1.2771
Model 1c	5.80	0.717	1.0164

3.2 Model 2e

The differences between Model 2e and Model 2d are:

- The first mode of vibration of the standing body is dominated by the upper part (head neck, upper torso and central torso) of the body. Two mass devices are presented in Model 2e with a magnitude of $M_{H1}-M_{H11}$ and $M_{H2}-M_{H22}$ respectively.
- The sum of the top and bottom masses is M_{H0} =1.0, in Model 2e, while the total mass in model mass in Model 2d is 0.0909+0.655+0.254 =0.9999.
- Following the same method presented in Section 3.1, the apparent mass for Model 2e is:

$$M_{2e}(i\omega)=\frac{M_{H1}((\frac{M_{H1}}{M_{H11}}-1)(2\pi f)^2+i2\xi_{H1}(2\pi f_{H1})(2\pi f)+(2\pi f_{H1})^2)}{(-(2\pi f)^2+i2\xi_{H1}(2\pi f_{H1})(2\pi f)+(2\pi f_{H1})^2)}+\frac{M_{H2}((\frac{M_{H2}}{M_{H22}}-1)(2\pi f)^2+i2\xi_{H2}(2\pi f_{H2})(2\pi f)+(2\pi f_{H2})^2)}{(-(2\pi f)^2+i2\xi_{H2}(2\pi f_{H2})(2\pi f)+(2\pi f_{H2})^2)}+1-M_{H1}-M_{H2} \quad (20)$$

Following the same identification process as Model 1c, 3.2% of the total mass is assigned to the bottom mass in the parameter identification, i.e. $M_{H0}-M_{H1}-M_{H2}=3.2\%M_{H0}$ for model 1c or $M_{H0}+M_{H11}+M_{H22}-2M_{H1}-2M_{H2}=3.2\%M_{H0}$ for Model 2e, it is found that the identified results are not in a reasonable range.

The apparent mass of model 2d can be rewritten as follows:

$$M_{2d}(i\omega)=\frac{M_1(i2\xi_{H1}(2\pi f_{H1})(2\pi f)+(2\pi f_{H1})^2)}{(-(2\pi f)^2+i2\xi_1(2\pi f_{H1})(2\pi f)+(2\pi f_{H1})^2)}+\frac{M_2(i2\xi_{H2}(2\pi f_{H2})(2\pi f)+(2\pi f_{H2})^2)}{(-(2\pi f)^2+i2\xi_{H2}(2\pi f_{H2})(2\pi f)+(2\pi f_{H2})^2)} \quad (21)$$

Comparing Equation 20 and 21, it can be noted that two additional items, $(M_{H1}/M_{H11}-1)(2\pi f)^2$, $(M_{H2}/M_{H22}-1)(2\pi f)^2$, are present in the numerator in Equation 20. When the ratios M_{H1}/M_{H11} and M_{H2}/M_{H22} are given, the format of the two equations becomes the same.

Case 1: Let M_{H1}/M_{H11} =1.36, M_{H2}/M_{H22} =0.61 based on the continuous body model [4], the identified results are shown in Table 4.

The bottom mass becomes $M_{H0}-M_{H1}-M_{H2}$ $=1-0.484-0.562=-0.046<0$.

Physically the value of the bottom mass should be positive, hence this is not a valid case. But the same

phenomena can be observed as for Model 1c. The parameters M_{H1}/M_{H11} and M_{H2}/M_{H22} are constants (0.66 and 0.34), when M_{H1}/M_{H11} and M_{H2}/M_{H22} are changed during the identification process.

Therefore, the two parameters ${M_{H1}}^2/M_{H11}$ and ${M_{H2}}^2/M_{H22}$ are identified. So the parameter can be calculated by giving either, M_{H1} and M_{H2}, or, M_{H11} and M_{H22}.

Case 2: If M_{H1}=0.533, M_{H2}=0.296， based on the continuous body model[4], the identified results are shown in Table 4.

For Case 2, $M_{H2}(0.296) > M_{H22}(0.256)$, which is different from the characteristics of the continuous model, i.e. M_{H2} should be smaller than M_{H22}. Hence it is not a valid case.

Case 3: If M_{H11}=0.391, M_{H22}=0.487, based on the continuous body model[1], the identified results are shown in Table 4.

Table 4. Identified parameters of Model 2e

	M_{H1}	M_{H11}	f_{H1}	ξ_{H1}	M_{H2}	M_{H22}	f_{H2}	ξ_{H2}
Case 1	0.484	0.356	5.78	0.369	0.562	0.921	13.2	0.445
Case 2	0.533	0.431	5.78	0.369	0.296	0.256	13.2	0.445
Case 3	**0.507**	**0.391**	**5.78**	**0.369**	**0.409**	**0.487**	**13.2**	**0.445**

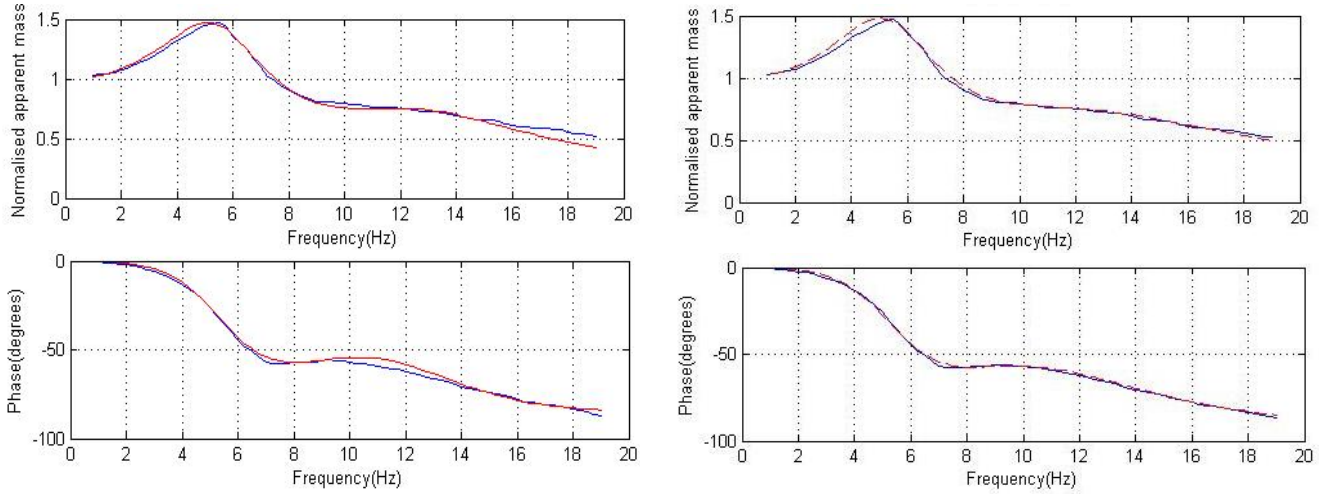

a) Model 2d *b) Model 2e*

Figure 2. Comparison of the normalized apparent masses and the phase between Models 2d and 2e

Table 5. Identified parameters of Model 2d and 2e

	f_{H1} (Hz)	ξ_{H1}	f_{H2} (Hz)	ξ_{H2}	error
Model 2d	5.88	0.364	13.5	0.330	0.1573
Model 2e	5.78	0.369	13.2	0.445	0.0595

For case 3, Fig. 2 compares the measured and identified normalised apparent mass and the phase against frequency of Model 2d and 2e, where the solid lines indicate the measurements and the dashed lines indicate the theoretical predictions.

The results in Table 5 and Fig. 2 show that:

- f_{H1} and f_{H2} of Model 2e are slightly smaller than those of Model 2d, while ξ_{H2} of Model 2e is greater than that of Model 2d.
- The dynamic properties of Models 2d obtained from Equations 4 are the same as that quoted from [3], which verifies that the curving fitting procedure and equations used in this study are correct.
- The interaction model (Models 2e) provides smaller fitting errors than Model 2d [1], which may indicate that the interaction model is more appropriate representations of a standing human body than Model 2d.
- As Model 2d and 2e are physically different, it is expected that the basic parameters of the two models would have some differences although they are determined from the same sets of measurements.

4 Comparison of the Human-Structure Models

It is necessary to assess whether parameters of the human body models, Model 1c and Model 2e are correct. For verification, the continuous body model [1] and the two newly derived models (Model 1c and Model 2e) are placed on a SDOF structure model to form human-structure models as shown in Fig. 3. The eigenvalue analyses of the human-structure models are calculated for comparison.

The human-structure models in Fig. 3 are explained as follows with each model being placed on the same SDOF structural model:

H-S Model 1: The continuous human body has seven different mass densities distributed over the height of the body. The two axial stiffnesses are assigned to the continuous body model [1] as shown in Fig. 3a. The stiffness k_1=134.9 kN/m is assigned to the four lower parts while k_2=24.01kN/m is assigned to the three upper parts[1].

H-S Model 2: Model 1b using the parameters determined by Matsumoto and Griffin [1].

H-S Model 3: Model 2d using the parameters in determined by Matsumoto and Griffin [1].

H-S Model 4: Model 1c using the parameters in Table 2.

H-S Model 5: Model 2e using the parameters in Table 4

The four body models in the last four H-S models are all abstracted from the same measured apparent mass. In the analysis, the parameters of the SDOF structure model are altered to obtain particular values

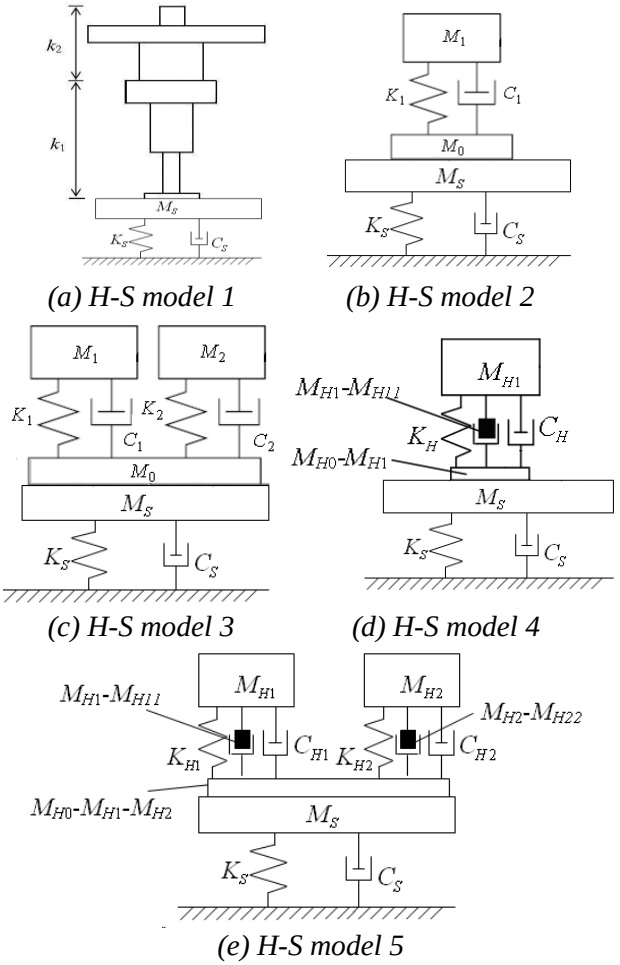

Figure 3. Human-structure models with different body models

of the ratio of the total body mass to the modal mass of the SDOF structure, $\eta = M_{H0} / M_S$, as are the values of the ratio of the fundamental natural frequency of the human-body to that of the SDOF structure $\beta = f_{H1} / f_S$. Choosing η = 0.01, 0.1 and 1.0 and β =0.5, 1.0 and 2.0 gives nine combinations. The eigenvalue analysis of H-S Model 1 (Model 3 on a SDOF structure) is conducted using ANSYS, while the natural frequencies of the other H-S Models are solved based on the exact mathematical expressions.

4.1 Comparison between the same Human-Structure Models using different parameters

As mentioned in Section 3.1 and 3.2, in order to know the effect of the different parameters, the three natural frequencies of H-S Models 4 and 5 with different parameters are listed in Table 6.

The comparison of the results in Table 6 shows that:

- When η is very small (η= 0.01), there is little difference between the natural frequencies of H-S Models 4 and 5.
- When η is small (η= 0.1), the corresponding natural frequencies of H-S Models 4 and 5 are similar.
- When η is large (η= 1.0), the difference between of H-S Model 4 and 5 becomes slightly larger when the order of the natural frequency increases.
- The three natural frequencies of H-S models 4 and 5 are unchanged with the different parameters based on the identified results.

Table 6. Comparison of the first three natural frequencies of a human-structure model using different body models

Human-Structure Models	η	0.01			0.1			1		
	f_S (Hz)	3	6	12	3	6	12	3	6	12
Fundamental natural frequency										
H-S Model 4	Case 1	2.98	5.60	5.79	2.82	5.04	5.71	2.05	3.66	5.10
	Case 2	2.98	5.60	5.79	2.82	5.04	5.71	2.05	3.66	5.10
H-S Model 5	Case 1	2.98	5.63	5.77	2.83	5.15	5.72	2.07	3.78	5.26
	Case 2	2.98	5.63	5.77	2.83	5.15	5.72	2.07	3.78	5.26
	Case 3	2.98	5.63	5.77	2.83	5.15	5.72	2.07	3.78	5.26
Second natural frequency										
H-S Model 4	Case 1	5.84	6.22	12.0	6.18	6.92	12.2	8.69	9.72	13.9
	Case 2	5.84	6.22	12.0	6.18	6.92	12.2	8.69	9.72	13.9
H-S Model 5	Case 1	5.81	6.14	11.9	6.01	6.59	11.4	7.09	7.62	9.94
	Case 2	5.81	6.14	11.9	6.02	6.60	11.4	7.09	7.62	9.95
	Case 3	5.81	6.14	11.9	6.01	6.59	11.4	7.09	7.62	9.94
Third natural frequency										
H-S Model 5	Case 1	13.2	13.2	13.3	13.4	13.5	14.1	15.6	15.9	17.5
	Case 2	13.2	13.2	13.3	13.4	13.5	14.1	15.6	15.9	17.5
	Case 3	13.2	13.2	13.3	13.4	13.5	14.1	15.6	15.9	17.5

For H-S Model 4, the equation of motion is:

$$\begin{bmatrix} M_S + M_{H0} + M_{H11} - 2M_1 & M_{H1} - M_{H_{11}} \\ M_{H1} - M_{H11} & M_{H11} \end{bmatrix} \begin{Bmatrix} \ddot{u}_s \\ \ddot{u}_{H1} \end{Bmatrix} + \begin{bmatrix} C_S + C_{H1} & -C_{H1} \\ -C_{H1} & C_{H1} \end{bmatrix} \begin{Bmatrix} \dot{u}_s \\ \dot{u}_{H1} \end{Bmatrix} + \begin{bmatrix} K_S + K_{H1} & -K_{H1} \\ -K_{H1} & K_{H1} \end{bmatrix} \begin{Bmatrix} u_s \\ u_{H1} \end{Bmatrix} = \begin{Bmatrix} 0 \\ 0 \end{Bmatrix} \tag{22}$$

The solution of Equation 22 without considering the damping terms leads to the expressions of the natural frequencies:

$$f_1^2 = \frac{f_s^2 + (1+\eta) f_H^2 - \sqrt{[f_s^2 + (1+\eta) f_H^2]^2 - 4(1+\eta-\gamma^2/\alpha) f_S^2 f_H^2}}{2(1+\eta-\gamma^2/\alpha)} \tag{23}$$

$$f_2^2 = \frac{f_s^2 + (1+\eta) f_H^2 + \sqrt{[f_s^2 + (1+\eta) f_H^2]^2 - 4(1+\eta-\gamma^2/\alpha) f_S^2 f_H^2}}{2(1+\eta-\gamma^2/\alpha)} \quad (24)$$

where:

$$\eta = \frac{M_{H0}}{M_S} \quad \alpha = \frac{M_{H11}}{M_S} \quad \gamma = \frac{M_{H1}}{M_S} \quad (25)$$

There are four parameters η, f_S, f_H, γ^2/α in Equation 25. The values of η and f_S are given for each case. The value of f_H and γ^2/α are identified in Tables 1~3. Interestingly, f_H and γ^2/α are the same value for both case 1 and case 2 of Model 1c. This would explain why the natural frequencies are unchanged with the different parameters for H-S Model 4. The reason for H-S Model 5 should be the same, although the expressions of the natural frequencies cannot be written directly.

4.2 Comparison between different Human-Structure Models

The natural frequencies of the H-S models 2, 3, 4 and 5 and the first three natural frequencies of the H-S model 1 with different mass ratios $\eta = M_{H0}/M_S$ and frequency ratios $\beta = f_{H1}/f_S$ are listed in Table 7.

Table 7. Comparison of the first three natural frequencies of H-S Model 4 and 5 with different parameters

Human-Structure Models	η	0.01			0.1			1		
	f_S (Hz)	3	6	12	3	6	12	3	6	12
Fundamental natural frequency										
H-S 1: Model 3		2.98	5.68	5.87	2.83	5.17	5.81	2.07	3.77	5.29
H-S 2: Model 1b		2.98	5.65	5.86	2.82	5.09	5.78	2.03	3.67	5.17
H-S 3: Model 2d		2.98	5.70	5.87	2.83	5.19	5.82	2.07	3.80	5.33
H-S 4: Model 1c		2.98	5.60	5.79	2.82	5.04	5.71	2.05	3.66	5.10
H-S 5: Model 2e		2.98	5.63	5.77	2.83	5.15	5.72	2.07	3.78	5.26
Second natural frequency										
H-S 1: Model 3		5.91	6.20	12.0	6.14	6.72	11.8	7.48	8.11	11.0
H-S 2: Model 1b		5.91	6.23	12.0	6.22	6.89	12.1	8.28	9.16	13.0
H-S 3: Model 2d		5.91	6.18	11.9	6.12	6.66	11.5	7.23	7.77	10.3
H-S 4: Model 1c		5.84	6.22	12.0	6.18	6.92	12.2	8.69	9.72	13.9
H-S 5: Model 2e		5.81	6.14	11.9	6.01	6.59	11.4	7.09	7.62	9.94
Third natural frequency										
H-S 1: Model 3		14.9	14.9	14.9	15.0	15.0	15.2	16.2	16.4	17.3
H-S 3: Model 2d		13.5	13.5	13.6	13.7	13.7	14.1	15.2	15.4	16.7
H-S 5: Model 2e		13.2	13.2	13.3	13.4	13.5	14.1	15.6	15.9	17.5

The comparison of the results in Table 7 shows that:

- When η is very small ($\eta = 0.01$), there is little difference between the natural frequencies of the last four H-S models.
- When η is small ($\eta = 0.1$), the corresponding natural frequencies from the last four models are similar.
- When η is large ($\eta = 1.0$), the difference between the Matsumoto's models and the interaction models becomes slightly larger when the order of the natural frequency increases.
- For the two DOF models (H-S Models 2 and 4), the following condition hold: $f_1 \le (f_S, f_H) \le f_2$.
- There are no obvious difference between the biomechanics and interaction models when $\eta \le 0.1$.

The interaction models show better agreements with the continuous model than the biomechanics models.

Especially, H-S Models 5 shows the best agreement with the H-S Model 1.

5 Conclusions

This paper determines the parameters of the proposed interaction body models (Fig. 2) using the available measurements of Matsumoto and Griffin. The conclusions drawn from this study are:

- Similar to the parametric identification of Matsumoto and Griffin, the parameters identified are not unique as one additional condition that has to be given for Models 1b and 2d. For the interaction models (Fig. 2), one additional condition is required for Model 1c and two conditions for Model 2e. This could lead to several sets of parameters, but with the results from the continuous model, reasonable parameters of the two interaction models are identified.
- The quality of the curve fitting for the interaction model is as good as (Model 1c) and is slightly better (Model 2e) than the published results (Models 1b and 2d).
- Based on Model 2e, f_1 is identified as 5.78Hz, and ξ_1 of the interaction model is 0.369. f_2 is identified as 13.2Hz, and ξ_2 of the interaction model is 0.445. These parameters can be used in further calculations.
- There are no obvious differences between the biomechanics and interaction models when $\eta \leq 0.1$.

Acknowledgements

The authors are grateful for the financial support of the National Natural Science Foundation of China (Grant No. 51508133); China Postdoctoral Science Foundation (Grant No. 2014M551255); Heilongjiang Postdoctoral Fund (Grant No. LBH-Z15089); Scientific Research Foundation for Returned Scholars, Ministry of Education of China.

References

[1] Matsumoto, Y., Griffin, M. J.: *Mathematical Models for the apparent masses of standing subjects exposed to vertical whole-body vibration*, Journal of Sound and Vibration, 260 (2003), 431-451.

[2] Griffin, M. J.: *Handbook of Human Vibration*, Academic Press, London, UK, 1990

[3] Matsumoto, Y., Griffin, M. J.: *Dynamic response of the standing human body exposed to vertical vibration: influence of posture and vibration magnitude*, Journal of Sound and Vibration, 212 (1998), 1, 85-107.

[4] Ji, T., Zhou, D., and Zhang, Q.: *Models of a standing human body in vertical vibration*, Proceedings of the Institution of Civil Engineers: Structures and Buildings, 166 (2013), 7, 367-378.

[5] Ji, T., Wang, D., Zhang, Q., & Duarte, E.: *Presence of Resonance Frequencies in a Heavily Damped Two-Degree-of-Freedom System*, Journal of Engineering Mechanics, 140 (2014), 2, 406-415.

[6] Zhang, Q., Zhang, Y., Ji, T.: *A Continuous Model of a Standing Human Body in Vertical Vibration*, Journal of Engineering Review, 2016, In press

[7] Bartz, J. A., Gianotti, C. R.: *Computer program to generate dimensional and inertial properties of the human body*, Journal of Engineering for Industry, 75 (1975), 49-57.

[8] Nigam, S. P., Malik, M.: *A study on a vibratory Model of a human body*, Journal of Biomechanical Engineering, 109 (1987), 148-153.

[9] Ji, T.: *A continuous Model for the vertical vibration of the human body in a standing position*, UK Informal Group Meeting on Human Response to Vibration, 1995, Silsoe, UK

[10] Wei, L., Griffin, M. J.: *Mathematical models for the apparent mass of the seated human body exposed to vertical vibration*, Journal of Sound and Vibration, 212 (1998), 5, 855-874.

Appendix

The meanings of notations in this paper are presented as follow:

C_{H1}, C_{H2} the modal damping coefficients of discrete human-body models

C_S the damping coefficient of a SDOF structure system

ξ_{H1}, ξ_{H2} the damping ratios of discrete human-body models

f_S (Hz) the natural frequency of a SDOF structure system

f_{H1}, f_{H2} (Hz) the first and second natural frequencies of a standing human body

k_1, k_2 (kN/m) the axial stiffnesses of the lower and upper parts of a bar

K_{H1}, K_{H2} (N/m) the modal stiffnesses of discrete human-body models

M_{H0} (kg) the whole-body mass

M_{H1}, M_{H2} (kg) the participating masses of the first and second modes of a human body respectively

M_{H11}, M_{H22} (kg) the modal masses of the first and second modes of a human body respectively

$u_H(x,t)$ (m) the absolute movement of a human body

$u_{H1}(t)$, $u_{H2}(t)$ (m) the absolute movements of the first and second modes of a human body

α the ratio of the modal mass of the first mode of the body to the modal mass of the structure

η the ratio of the whole body mass to the modal mass of the structure

γ the ratio of the participating mass of the first mode of the body to the modal mass of the structure

β the ratio of the natural frequency of the first mode of the body to the natural frequency of the SDOF structure system